Measurements of spontaneous-emission rates in atomic thallium

L. Hunter and E. Commins
Physics Department, University of California, Berkeley, California 94720
and Materials and Molecular Research Division, Lawrence Berkeley Laboratory, Berkeley, California 94720

L. Roesch
Laboratory for Nuclear Physics ETH, Zurich, Switzerland
(Received 6 July 1981)

We report measurements of the following spontaneous-emission rates in atomic thallium: $A(6D_{3/2}\text{-}7P_{1/2})=(5.97\pm0.78)\times10^5\ s^{-1}$, $A(7P_{1/2}\text{-}7S_{1/2})=(1.71\pm0.07)\times10^7\ s^{-1}$, $A(7P_{3/2}\text{-}7S_{1/2})=(2.37\pm0.09)\times10^7\ s^{-1}$, and $A(8P_{3/2}\rightarrow\text{all})=(9.2\pm1.0)\times10^6\ s^{-1}$. These results are compared to predictions of theoretical models and lend support to calculations of the recently measured parity-nonconserving circular dichroism of the $6P_{1/2}\text{-}7P_{1/2}$ forbidden $M1$ transition in thallium.

I. INTRODUCTION

The $6^2P_{1/2}\text{-}7^2P_{1/2}$ forbidden $M1$ transition in thallium is of considerable interest in connection with experimental observation of parity nonconservation due to neutral weak currents[1-3] (see Fig. 1). The transition is nominally forbidden $M1$ with amplitude $\mathcal{M}$, but there exists an additional parity-violating $E1$ amplitude $\mathcal{E}_P$, which leads to circular dichroism $\delta\simeq+2\,\mathrm{Im}\mathcal{E}_P/\mathcal{M}$. $\mathcal{M}$ is known from an interference experiment[4] which utilizes an external electric field E, and in which one measures $-2\mathcal{M}/\beta E$, $4\mathcal{M}/3\alpha E$, in the absorption $6^2P_{1/2}\rightarrow7^2P_{1/2}$. Here β is the Stark amplitude for linear polarization of absorbed radiation perpendicular to the applied electric field, given by

$$\beta=\tfrac{1}{9}\sum_{nS}R_{7P,nS}R_{nS,6P}\left[\frac{1}{E_{6P}-E_{nS}}-\frac{1}{E_{7P}-E_{nS}}\right]+\tfrac{1}{9}\sum_{nD_{3/2}}R_{7P,nD_{3/2}}R_{nD_{3/2},6P}\times\left[\frac{1}{E_{7P}-E_{nD_{3/2}}}-\frac{1}{E_{6P}-E_{nD_{3/2}}}\right],\tag{1}$$

where $E_{6P}=6^2P_{1/2}$ energy, etc.,

$$R_{7P,nS}=\langle 7^2P_{1/2}\,|\,r\,|\,n^2S_{1/2}\rangle\ ,$$

etc., and r is the electron radial coordinate. Also α is the Stark amplitude for linear polarization parallel to the electric field:

$$\alpha=\tfrac{1}{9}\sum_{nS}R_{7P,nS}R_{nS,6P}\left[\frac{1}{E_{7P}-E_{nS}}+\frac{1}{E_{6P}-E_{nS}}\right]+\tfrac{2}{9}\sum_{nD_{3/2}}R_{7P,nD_{3/2}}R_{nD_{3/2},6P}\times\left[\frac{1}{E_{7P}-E_{nD_{3/2}}}+\frac{1}{E_{6P}-E_{nD_{3/2}}}\right].\tag{2}$$

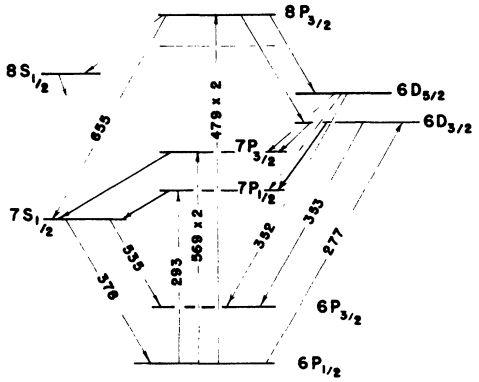

FIG. 1. Low-lying energy levels of thallium (not to scale). Wavelengths of relevant transitions are shown in nm.

Since α,β have never been measured directly, the determination of $\mathcal{M}$ depends on a reliable calculation of these quantities.[5]

Theoretical determination of the parity-violating amplitude $\mathcal{E}_P$ also requires evaluation of an infinite sum involving similar radial matrix elements, as well as zero-range parity-violating matrix elements:

$$\mathcal{E}_P=\sum_{nS}\frac{\langle 7P_{1/2}\,|\,E1\,|\,nS\rangle\langle nS\,|\,H_{\rm PV}\,|\,6P_{1/2}\rangle}{E_{6P}-E_{nS}}+\frac{\langle 7P_{1/2}\,|\,H_{\rm PV}\,|\,nS\rangle\langle nS\,|\,E1\,|\,6P_{1/2}\rangle}{E_{7P}-E_{nS}}\,, \tag{3}$$

where the factors $\langle nS\,|\,H_{\rm PV}\,|\,n'P\rangle$ depend on the electron wave functions and their derivatives at the nucleus. The electric dipole terms of the sum may be expressed as

$$\langle nS_{1/2}\,|\,E1\,|\,n'P_{1/2}\rangle=e\langle nS_{1/2}\,|\,\hat{\epsilon}\cdot\vec{r}\,|\,n'P_{1/2}\rangle=\frac{e}{3}R_{nS,n'P}\,.$$

It is clear that accurate values of the radial matrix elements $R_{nS,n'P}$ and $R_{nD_{3/2},n'P}$ are required for a precise theoretical estimate of δ.

The A coefficient between a $P_{1/2}$ state and either a $D_{3/2}$ or $S_{1/2}$ state may be expressed as

$$A=\tfrac{4}{9}e^2R^2_{nP,n'D,n'S}\,|\,E_{nP}-E_{n'D,n'S}\,|^3\,.$$

The $7\,^2S_{1/2}$ and $6\,^2D_{3/2}$ states play a dominant role in the sums of Eqs. (1)–(3).[5] $A(7S_{1/2}\text{-}6P_{1/2})$ and $A(6D_{3/2}\text{-}6P_{1/2})$ are already known.[6] We here describe measurements of $A(6D_{3/2}\text{-}7P_{1/2})$, $A(7P_{1/2}\text{-}7S_{1/2})$, $A(7P_{3/2}\text{-}7S_{1/2})$, and $A(8P_{3/2}\rightarrow\text{all})$. The measurements provide a good test of the large r behavior of calculated excited-state wave functions. In all measurements we employ thallium with the natural abundance (29.5% $T1^{203}$ and 70.5% $T1^{205}$). Both isotopes possess nuclear spin $I=\frac{1}{2}$.

II. EXPERIMENTAL METHOD AND RESULTS

A. $7P_{1/2}$ lifetime

We measure the $7P_{1/2}$ lifetime by observation of the Hanle effect. Circularly polarized laser light tuned to the $6P_{1/2}\rightarrow 7P_{1/2}$ transition at 292.7 nm travels along $\hat{x}$ in thallium vapor, as shown in Fig. 2. An electric field $\vec{E}$ along $\hat{y}$ induces Stark electric dipole absorption amplitudes αE and βE. When the laser is tuned to the $F=1\rightarrow F'=1$ hyperfine transition, interference between α and β amplitudes causes a polarization along $\hat{x}$:

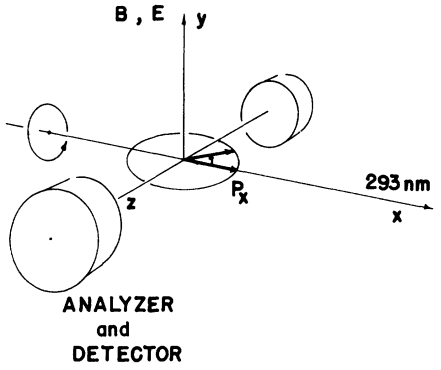

FIG. 2. Schematic of experimental arrangement for $7P_{1/2}$ lifetime measurement. With appropriate modifications described in the text, the same experimental arrangement was employed for $7P_{3/2}$ and $8P_{3/2}$ lifetimes.

$$P_x=\pm\frac{4\alpha\beta}{3\alpha^2+2\beta^2}\simeq\pm 0.74\,, \tag{4}$$

where $\pm$ refers to laser photon helicities ± 1. A weak magnetic field B along y causes P_x to precess in the x-z plane at a rate $\omega=g_F\mu_0B/\hbar$, where μ_0 is the electron Bohr magneton and g_F is the Lande g factor of the state. Photomultipliers along $\pm z$ detect the left circularly polarized ($h=+1$) component of the $7S_{1/2}$-$6P_{3/2}$ decay fluorescence at 535.0 nm. This fluorescence originates from cascade decays $7P_{1/2}\rightarrow 7S_{1/2}\rightarrow 6P_{3/2}$ or from conversion of resonantly trapped 378-nm radiation ($7S_{1/2}$-$6P_{1/2}$). See Fig. 1.

The cascade process dilutes the original polarization by a factor of 6. An additional factor is lost because of resonance trapping, imperfect polarization analysis, and imperfect initial polarization of the 292.7-nm light.

It may be shown that the observed circular polarization is given by the formula

$$\langle P_z\rangle 535\text{ nm}=\frac{b(a+a')}{(1+a^2)(1+a'^2)}\,, \tag{5}$$

where

$$a'=\frac{eB}{2m_ecA(7S)_{\rm tot}}\,,\quad a=\frac{eB}{6m_ecA(7P_{1/2})}\,,$$

and $b=$ overall analyzing power. In order to determine $A(7P_{1/2}\text{-}7S_{1/2})$ we measure $\langle P_z\rangle$ vs B. The overall scale factor b is unimportant for the determination of $A(7P_{1/2}\text{-}7S_{1/2})$. Only the shape

of the curve and, in particular, the position of the maximum is crucial. From previous measurements,[6]

$$A(7S\rightarrow\text{all})=(13.3\pm0.3)\times10^7\ , \tag{6}$$

in units of s^{-1}.

The 292.7 nm is generated using the same technique and equipment described in a previous publication.[3,7] Circular polarizations of opposite helicities are produced with a carefully aligned quartz-quarter wave plate (Virgo Optics) mounted on a precision 180° rotator which flips the quarter wave plate about an axis at 45° to both the fast and slow optic axes.

A sealed off quartz thallium cell was utilized for all measurements reported here. The cell is surrounded by a large stainless-steel oven mounted inside a crude vacuum. A separate "stem" heater surrounds a quartz protrusion from the bottom of the cell where the thallium condenses. The stem heater is used to control the thallium density.

The cell is supported from below by a grounded stainless-steel electrode external to the cell. A pulsed voltage of 600 V is applied to a second stainless-steel electrode which rests on top of the cell, 12.5 mm above the grounded plate. The polarization P_x [Eq. (4)] is independent of the amplitude of the electric field and hence no precise calibration of the electric field is required.

The magnetic field is produced by a pair of Helmholtz coils with 43-cm diameter. The magnetic field increases linearly with the applied voltage according to

$$B(\text{G})=B_0+(3.80\pm0.04)\text{V(volts)} \tag{7}$$

and varies by less than 0.5% over the fiducial volume as measured with three calibrated Hall probes.[7]

The data were taken at various sequences of magnetic field settings. At each magnetic field setting, four signals, each summed over 400 laser pulses in a gated dual scaler, were stored: S_{1+}, S_{1-}, S_{2+}, and S_{2-}. The subscripts 1 and 2 refer to the fluorescence signals observed in phototubes 1 and 2 (along the $\pm z$ axis in Fig. 1) while the + and − refer to the incident uv helicity. The asymmetry P_{Han}, corrected for intensity fluctuations and analyzing power, is then calculated:

$$P_{\text{Han}}=\frac{1-z}{1+z}\ ,$$

where

$$z=\sqrt{(S_{1+}/S_{1-})/(S_{2+}/S_{2-})}\ .$$

We define a quantity K which allows for a systematic offset in the quantity P_{Han} due to a systematic intensity difference between the various configurations. The quantities P_{Han}-K are fit to the function (5) using Eqs. (6) and (7). There are then four parameters: b, B_0, K, and $A(7P_{1/2}$-$7S_{1/2})$, which are fit to the data. The low-density data ($n\leq2\times10^{12}$ cm^{-3}) is very consistent. The high-density data ($n\geq10^{14}$ cm^{-3}) show a slight decrease in the lifetime of the $7P_{1/2}$ state. The analyzing power (b) also falls off at a higher density indicating a depolarization due either to collisions or resonance trapping of the 378-nm radiation to the ground state. We therefore include only the low-density data (i.e., data with stem temperatures less than 850 K corresponding to $n\leq2\times10^{13}$ cm^{-3}) in our final analysis. Combining these data we find

$$A(7P_{1/2}\text{-}7S_{1/2})=(1.71\pm0.07)\times10^7 \tag{8}$$

s^{-1}, in units of where we have included the uncertainty in $A(7S_{1/2}\rightarrow\text{all})$ and in B as well as the statistical uncertainty.

This may be compared to the theoretical values

$$A(7P_{1/2}\text{-}7S_{1/2})=1.88\times10^7$$

(Ref. 5) and

$$A(7P_{1/2}\text{-}7S_{1/2})=1.64\times10^7\ ,$$

both in units of s^{-1}.[8]

B. $7P_{3/2}$ lifetime

A measurement of the $7P_{3/2}$ lifetime was also made using a method similar to that outlined in Sec. II B. The transition $6P_{1/2}(F=0)\rightarrow7P_{3/2}$ $(F=2)$ was excited using two circularly polarized photons at 568.8 nm. The light was generated using Rhodamin 110 dye and was polarized using a 140-nm polaroid plastic retardation plate. This procedure produces an almost complete initial polarization of the $7P_{3/2}$ state. Because of the high rate associated with the two-photon transition care must be taken to avoid stimulated emission.

The physical mechanism operating here may be explained as follows. A ground-state atom $(6^2P_{1/2},F=0)$ absorbing two photons, each of helicity +1, reaches the $(7^2P_{3/2},F=2,m_F=+2)$ level at $t=0$. The atom immediately begins to precess in the external magnetic field, so that at some later time t it is in a coherent superposition of the various m_F components of the $F=2$ state. However,

the $m_F=+2$ component is strongly coupled to the ground state by a sufficiently intense laser field (two-photon stimulated emission) and therefore this component may be depleted appreciably. The result (which we have analyzed in detail by integrating the appropriate coupled differential equations) is a shortening of the lifetime of $7\,^2P_{3/2}$ which depends on the magnetic field, and thus distorts the Hanle curve as well as changing its peak value.

As in the measurement of the $7P_{1/2}$ lifetime, fluorescence at 535 nm was observed. The results were fit to the function of Eq. (5) with

$$a=\frac{eB}{2m_e cA(7P_{3/2})},\quad K=0\ .$$

A fit was also performed with $K\neq 0$ with similar results. Folding in the stated uncertainties in B and $A(7S_{1/2})$, the results are

$$A(7P_{3/2}\text{-}7S_{1/2})=(2.37\pm 0.09)\times 10^7 \tag{9}$$

in units of s^{-1}, which may be compared to the theoretical predictions

$$A(7P_{3/2}\text{-}7S_{1/2})=2.37\times 10^7$$

(Ref. 5) and

$$A(7P_{3/2}\text{-}7S_{1/2})=2.11\times 10^7\ ,$$

both in units of s^{-1}.[8]

C. $8P_{3/2}$ lifetime

Measurement of the $8P_{3/2}$ lifetime was carried out in a similar manner. The transition $6P_{1/2}(F=0)\rightarrow 8P_{3/2}(F=2)$ was excited using two 479-nm circularly polarized photons generated with LD473 dye (Exciton Corp.), and the same polaroid retardation plate as in Sec. II B. The polarization of the subsequent fluorescence was observed in both 655 ($8P_{3/2}\rightarrow 7S_{1/2}$), 353, and 352 nm ($8P_{3/2}\rightarrow 6D_{3/2,5/2}\rightarrow 6P_{3/2}$). Observations at 353 and 352 nm were made to circumvent the blackbody backgrounds at 655 nm.

The measurements at 655 nm were fit to function (5) with

$$a=\frac{eB}{2m_e cA(7P_{3/2})}$$

and

$$a'=0\ ,$$

while for the measurements at 353.0 nm,

$$a'=f_{D_{3/2}}\left[\frac{63}{75}\,\frac{eB}{2m_e cA(6D_{3/2})}\right]+f_{D_{5/2}}\left[\frac{77}{75}\,\frac{eB}{2m_e cA(6D_{5/2})}\right],$$

where $f_{D_{3/2,5/2}}$ are the fractions of the observed intensities at 353 and 352 nm. We take $f_{D_{3/2}}=0.09$ and $f_{D_{5/2}}=0.91$, while from earlier measurements[6]

$$A(6D_{3/2}\rightarrow\text{all})=(14.8\mp 1.1)\times 10^7$$

and (10)

$$A(6D_{5/2}\rightarrow\text{all})=(12.4\mp 1.3)\times 10^7\ ,$$

both in units of s^{-1}. The precession is very insensitive to the precise value of $f_{D_{3/2,5/2}}$ and $A(6D_{3/2,5/2})$ because the electron typically remains less than 7% of the time in the intermediate D state.

Due to a near cancellation in the contribution to the two-photon amplitude from the intermediate $S_{1/2}$ and $D_{3/2}$ states, the excitation rate is suppressed by approximately three orders of magnitude compared to the two-photon rate to $7P_{3/2}$. In order to compensate for the large original reduction it was necessary to operate with a tighter focus of the incident beam than was used in the $7P_{3/2}$ measurement. It was thus impossible to completely eliminate stimulated emission effects. The stimulated emission, besides shortening the observed lifetime, produces an easily observable signal asymmetry. A decrease in signal occurs which is largest for zero magnetic field and is less at large fields due to the selective depletion of the populated $F=2$, $m_F=2$ level by the stimulated emission. Application of a large field allows the state to rotate before it may be stimulated to emit. We may thus sense the presence and magnitude of the stimulated emission by observing the intensity difference between small and large magnetic fields. This effect has been observed experimentally, calculated exactly in various limits, and calculated numerically for cases of interest. It is possible using these results to correct for the effect of stimulated emission on the lifetime. We summarize here only the results where this correction was less than 10% and where the density was sufficiently low to avoid collisional effects. Approximately one-half of the quoted error is due to uncertainty in the stimulated emission corrections. Folding in the statistical uncertainties and systematic uncertainties associated with the intermediate D states and the

magnetic field calibration we arrive at a final measurement:

$$A(8P_{3/2}\rightarrow\text{all})=(9.2\pm1.0)\times10^{6}\ , \tag{11}$$

in units of s^{-1}. This result may be compared to the prediction $A(8P_{3/2}\rightarrow\text{all})=7.72\times10^{6}\ s^{-1}$.[8]

D. Determination of $A(6D_{3/2}\text{-}7P_{1/2})$

We measure $A(6D_{3/2}\text{-}7P_{1/2})$ by exciting the $6P_{1/2}\text{-}6D_{3/2}$ transition and observing the ratio of the decay fluorescences at 378 and 353 nm. The A coefficient may be expressed in terms of this ratio and other better known rates in thallium:

$$A(6D_{3/2}\rightarrow7P_{1/2})=\frac{A(6D_{3/2}\text{-}6P_{3/2})A(7S)_{\text{tot}}}{U\times A(7S_{1/2}\text{-}6P_{1/2})}$$

$$-A(6D_{3/2}\text{-}7P_{3/2})\ , \tag{12}$$

where $U=I_{353\,\text{nm}}/I_{378\,\text{nm}}$ is the observed intensity ratio corrected for detector efficiency. A schematic of the apparatus used in this measurement is shown in Fig. 3.

Light at 558 nm is generated using Coumarin 540 dye (Exciton Corp.). An 80% reflecting output coupler is used to minimize shot-to-shot fluctuations. The power output is about 2 mJ/pulse at a repetition rate of about 10 Hz. The frequency is doubled in an INRAD *AD*P* crystal maintained at $T=100\,^{\circ}\text{C}$ to produce the 277-nm light. The subsequent fluorescence, collimated by two 1-in. quartz f-1 lenses, is simultaneously observed by a Jarrel-Ash $\frac{1}{2}$-m monochromator with 3.0-mm slits viewed with an RCA 8575 phototube, and an EMI 9780 phototube with a 353-nm interference filter. The broadband acceptance of the monochromator is chosen to enhance light collection and minimize wavelength setting errors.

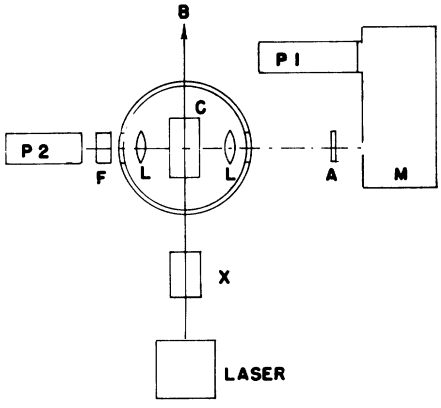

FIG. 3. Schematic of apparatus used in measuring $A(6D_{3/2}\text{-}7P_{1/2})$: A, optical attenuator; B, laser beam; C, cell; $P1$,$P2$, phototubes; M, monochromator; L, lenses; F, optical filter; X, doubling crystal.

The signal sizes are digitized, stored, and analyzed with an on-line LSI-11 computer system. The monochromator is tuned back and forth between 378 and 353 nm while the phototube viewing 353 nm is used to normalize the signals. When observing 353 nm an optical attenuator is inserted before the monochromator slit to approximately equalize the observed light intensities between 353 and 378 nm. The normalized ratio of the signal in 353 nm with attenuator to 378 nm without the attenuator is then measured. Data are taken at thallium vapor densities between $10^{10}-10^{11}\ \text{cm}^{-3}$. These low densities are chosen to avoid resonance trapping of 277- and 378-nm light. In addition, measurements are made at different positions in the cell and from each of the two ground-state hyperfine components. Data from all configurations agree very well, indicating that resonance trapping and background effects are of no significance. Calibration of the relative detection efficiencies of 378 and 353 nm with the optical filter is accomplished by replacing the thallium cell with an NBS calibrated 1000-W quartz-iodine lamp. The final value for U is

$$U=77\pm4\ , \tag{13}$$

where the error is entirely systematic: 3% in the measurement and 2% in the normalization. Using Eq. (12), the measured values of A coefficients to $6P_{1/2}$ and $6P_{3/2}$ states, and a theoretical value (Ref. 5) (with much larger fractional uncertainty) for the small A coefficient, $A(6D_{3/2}\rightarrow7P_{3/2})$, one

TABLE I. Experimental and theoretical values of A coefficients.

	These experiments $10^{7}\ s^{-1}$	Theory Ref. 5 $10^{7}\ s^{-1}$	Theory Ref. 8 $10^{7}\ s^{-1}$
$A(7P_{1/2})$	1.71 ±0.07	1.88	1.64
$A(7P_{3/2})$	2.37 ±0.09	2.37	2.11
$A(8P_{3/2}\rightarrow\text{all})$	0.92 ±0.10		0.772
$A(6D_{3/2}\rightarrow7P_{1/2})$	0.0597±0.0078	0.0479	0.0441

obtains

$$A(6D_{3/2}\rightarrow 7P_{1/2})=(5.97\pm 0.78)\times 10^5\ , \qquad (14)$$

in units of s^{-1}. This may be compared with the theoretical values of $4.79\times 10^5\ s^{-1}$ (Ref. 5) and $4.41\times 10^5\ s^{-1}$.[8]

The results and theoretical predictions, summarized in Table I, show reasonably good agreement.

ACKNOWLEDGMENTS

We thank P. Bucksbaum for his collaboration in the earlier stages of this work. This work was supported by the Director, Office of Energy Research, Office of Basic Energy Sciences, Chemical Sciences Division of the U. S. Department of Energy under Contract No. W-7405-ENG-48.

[1]R. Conti, P. Bucksbaum, S. Chu, E. Commins, and L. Hunter, Phys. Rev. Lett. 42, 343 (1979).

[2]P. Bucksbaum, E. Commins, and L. Hunter, Phys. Rev. Lett. 46, 640 (1981).

[3]P. Bucksbaum, E. Commins, and L. Hunter, Phys. Rev. D 24, 1134 (1981).

[4]S. Chu, E. Commins, and R. Conti, Phys. Lett. 60A, 96 (1977).

[5]D. Neuffer and E. D. Commins, Phys. Rev. A 16, 844 (1977).

[6]A. Gallagher and A. Lurio, Phys. Rev. A 136, 87 (1964).

[7]S. Chu and R. W. Smith, Opt. Commun. 28, 221 (1979).

[8]J. N. Bardsley and D. W. Norcross, J. Quant. Spectrosc. Radiat. Transfer 23, 575 (1980).